Journal of Applied Sciences 8 (19): 3361-3370, 2008
ISSN 1812-5654

Application of UNO Scheme for Steady and Transient Compressible Flow in Pressure-Based Method

M.H. Djavareshkian and M. Farnak
Department of Mechanic Engineering, Tabriz University, Tabriz, Iran

Abstract: A pressure based implicit procedure to solve the Euler equations on a nonorthogonal mesh with collocated finite volume formulations is described which uses pressure as a working variable. The boundedness criteria for this procedure are determined from Uniformly high order accurate Non Oscillatory (UNO) schemes, which are based on characteristic variables and are applied to the fluxes of the convected quantities directly, including mass flow rate. The developed scheme is applied to the computation of steady transonic and supersonic flow over a bump in channel geometry for various Mach number as well as to the transient shock tube problem. Also the results of steady supersonic flow over a ramp are presented. Then the results are compared with data predicted by TVD schemes based on characteristic variables.

Key words: High resolution, finite volume, UNO, total variation diminishing, transient, supersonic

INTRODUCTION

The capturing of sharp gradients associated with shock waves and contact discontinuities has been the subject of much research and development. In shock-capturing approach the governing equations of inviscid flows (Euler equations) are cast in conservation form and any shock waves or discontinuities are computed as part of the solution.

From an historical point of view, shock-capturing methods can be classified into two general categories: viz., classical methods and modern shock capturing methods (also called high-resolution schemes). Modern shock-capturing methods are generally upwind based in contrast to classical symmetric or central discretization. Upwind-type differencing schemes attempt to discretize hyperbolic partial differential equations by using differencing biased in the direction determined by the sign of the characteristic speeds. On the other hand, symmetric or central schemes do not consider any information about the wave propagation in the discretization.

No matter what type of shock-capturing scheme is used, a stable calculation in presence of shock waves requires a certain amount of numerical dissipation, in order to avoid the formation of unphysical numerical oscillations. In the case of classical shock-capturing methods, numerical dissipation terms are usually linear and the same amount is uniformly applied at all grid points. Classical shock-capturing methods only exhibit accurate results in the case of smooth and weak-shock solution, but when strong shock waves are present in the solution, non-linear instabilities and oscillations can arise across discontinuities. In other word, classical shock-capturing methods have the disadvantages that unphysical oscillations (Gibbs phenomenon) may develop in the vicinity of strong shocks.

Modern shock-capturing methods have, however, a non-linear numerical dissipation, with an automatic feedback mechanism which adjusts the amount of dissipation in any cell of the mesh, in accord to the gradients in the solution. These schemes have proven to be stable and accurate even for problems containing strong shock waves. Some of the well known classical shock-capturing methods include the MacCormack method, Lax-Wendroff method and Beam-Warming method. Also, there are many methods of modern shock-capturing schemes that between of them can be referred to TVD, ENO and UNO schemes.

The first is higher order Total Variation Diminishing (TVD) schemes that first proposed by Harten (1997). The TVD schemes are designed to posses their total variation diminishing property for scalar hyperbolic conservation laws and constant coefficient systems of hyperbolic conservation laws.

One of the disadvantages of TVD schemes is that they be switched to the first_order schemes in discontinuities. So they smeared the shocks and other discontinuities.

Recently, some researches have been accomplished in the devising of various high resolutions bounded schemes that based on the Total Variation Diminishing (TVD) technique and mostly they are oscillation free.

Corresponding Author: M.H. Djavareshkian, Department of Mechanic Engineering, Tabriz University, Tabriz, Iran
Tel: +984113392467

Druguet and Zeitoun (2003) used different MUSCL-TVD finite volume schemes to study the influence of the wedge trailing edge corner angle of the numerical methods and of the viscous effects on the shock wave reflections and on the hysteresis behavior. Sohn (2005) presented a new type of Eulerian MUSCL scheme and oscillation free algorithm based on TVD method. In his method, the inter cell flux is computed from difference approximation of characteristic equations.

Kim and Kim (2005) derived a new multi dimensional limiting function for an oscillation control in multi dimensional flows through the analysis of conventional TVD limiters. Also, they developed multi dimensional limiting process (MLP) with the multi dimensional limiting function. Mandal and Subramanian (2008) explored a novel technique of obtaining high resolution, second order accurate, oscillation free, solution dependent weighted least-squares (SDWLS) reconstruction in finite volume method. They explained an approach to verify TVD criterion of the SDWLS formulation for different choice of weights. They proposed a link between the solution dependent weights for weighted least squares formulation and various independently proposed limiter functions. Lian *et al.* (2008) proposed an improved r-factor algorithm for TVD schemes on structured and unstructured grids within a finite volume method framework for numerical approximation to the convective term. Kumar and Kadalbajoo (2008) presented a general procedure to construct a class of simple and efficient high resolution total variation (TVD) schemes for non linear hyperbolic conservation laws by introducing anti-diffusive terms with the flux limiters. Sokolov *et al.* (2006) generalized a TVD principle for a special case of piece-wise uniform grids, i.e., adaptive Cartesian grids.

Also, there is various Essentially Non-Oscillatory schemes (ENO) that first proposed by Harten *et al.* (1997). This scheme based on piece wise interpolating functions reinstructed in form of polynomials. The ENO scheme do not have a Gibbs_like phenomenon O (1) at discontinuities, yet they many occasionally produce small spurious oscillation on the level O (h^r) of the truncation error. Titarev and Toro (2005) proposed to use second order TVD fluxes, instead of first order monotone fluxes, in the framework of finite volume weighted essentially non oscillatory (WENO) schemes. They called the new improved schemes the WENO-TVD schemes. Shen *et al.* (2006) proposed a finite compact (FC) difference scheme requiring only bi_diagonal matrix inversion by using the known high resolution flux. Introducing TVD or ENO limiters in the numerical flux, they developed several high resolution FC-schemes of hyperbolic conservation law, including the FC-TVD, third order FC-ENO and fifth order FC-ENO scheme. Capdeville (2008a) proposed a new WENO procedure to compute multi-scale problems with embedded discontinuities, on non uniform meshes. He adapted this procedure for the non linear weights to maintain the theoretical convergence properties of the optimum reconstruction. Also Capdeville (2008b) proposed a new WENO procedure to compute problems containing both discontinuities and a large disparity of characteristic scales.

Other examples of modern shock-capturing schemes include, Flux-corrected Transport scheme introduced by Boris and Book (1997), Monotonic Upstream-centered Schemes for Conservation Laws (MUSCL) based on Godunov approach and introduced by van Leer (1997) and Piecewise Parabolic Method (PPM) proposed by Colella and Sekora (2008). Another important class of high resolution schemes belongs to the approximate Riemann solvers proposed by Roe (1997) and Shu and Osher (1989).

Uniformly high order accurate Non Oscillatory schemes (UNO) is another non oscillatory shock capturing methods for the approximation of hyperbolic conservation laws. These schemes share many desirable properties with total variation diminishing schemes, but TVD schemes have a most first order accuracy, in the sense of truncation error, at extrema of the solution. But in uniformly second order approximation, which is non oscillatory in the sense that the number of extrema of the discrete solution is not increasing in time. This is achieved via a non oscillatory piece wise linear reconstruction of the solution from its cell average, time evolution through an approximate solution of the resulting initial value problem and an average of this approximate solution over each cell.

So far, the UNO scheme has been used in density based algorithm. This imposes a restriction on the applicability of the methodology and precludes its use in multipurpose computational fluid dynamics procedures that can be applied to incompressible as well as compressible flows. Alternatively pressure-based methods offer the capability of handing both of these classes of flow in unified manner. The objection of this paper is to implement an Uniformly high order accurate Non Oscillatory schemes (UNO) with characteristic variables based flux limiters into a pressure based finite volume method that solves the Euler equations.

MATERIALS AND METHODS

Governing equations: The basic equations which describe conservation of mass, momentum and scalar quantities, can be expressed in Cartesian tensor form as:

$$\frac{\partial \rho}{\partial t}+\frac{\partial \left(\rho u_j\right)}{\partial x_j}=0 \qquad (1)$$

$$\frac{\partial(\rho U_i)}{\partial t}+\frac{\partial\left(\rho U_i U_j - T_{ij}\right)}{\partial x_j}=S_i^u \tag{2}$$

$$\frac{\partial(\rho\phi)}{\partial t}+\frac{\partial\left(\rho u_j\phi - q_j\right)}{\partial x_j}=S^\phi \tag{3}$$

The stress tensor and scalar flux vector are usually expressed in terms of basic dependent variables. The stress tensor for a Newtonian fluid is:

$$T_{ij}=-P\delta_{ij}-\frac{2}{3}\mu\frac{\partial u_k}{\partial x_k}\delta_{ij}+\mu\left(\frac{\partial u_i}{\partial x_j}+\frac{\partial u_j}{\partial x_i}\right) \tag{4}$$

The scalar flux vector is usually given by the Fourier type law:

$$q_j=\Gamma_\phi\left(\frac{\partial\phi}{\partial x_j}\right) \tag{5}$$

Discretization: The discretizations of the above differential equations are carried out using a finite volume approach. First, the solution domain is divided into a finite number of discrete volumes or cells, where all variables are stored at their geometric centers. The equations are then integrated over all the control volumes by using the Gaussian theorem. The development of the discrete expressions to be presented is affected with reference to only two face of the control volume, namely e and w, for the sake of brevity (Fig. 1). For any variable ϕ (which may now also stand for the velocity components), the result of the integration yields:

$$\delta v\frac{(\rho\phi)^{n+1}-(\rho\phi)^n}{\Delta t}+\underbrace{F_e\phi_e}_{I_e^C}-\underbrace{F_w\phi_w}_{I_w^C}=\underbrace{D_e\left(\phi_E^{n+1}-\phi_P^{n+1}\right)}_{I_e^D}-\underbrace{D_w\left(\phi_P^{n+1}-\phi_W^{n+1}\right)}_{I_w^D}+S_\phi\delta v \tag{6}$$

And continuity equation will be:

$$\delta v\frac{(\rho)^{n+1}-(\rho)^n}{\Delta t}+F_e-F_w=0 \tag{7}$$

With multiplying Eq. 7 in ϕ_p^{n+1} and minus of Eq. 6:

$$\delta v\frac{\rho^n\left(\phi_P^{n+1}-\phi_P^n\right)}{\Delta t}+\left(I_e^c-F_e\phi_P^{n+1}\right)-\left(I_w^c-F_w\phi_P^{n+1}\right)=\underbrace{D_e\left(\phi_E^{n+1}-\phi_P^{n+1}\right)}_{I_e^D}-\underbrace{D_w\left(\phi_P^{n+1}-\phi_W^{n+1}\right)}_{I_w^D}+S_\phi\delta v \tag{8}$$

And for two dimensional flow:

$$\delta v\frac{\rho_p^n\left(\phi_P^{n+1}-\phi_P^n\right)}{\Delta t}+\left(I_e^D+I_e^C-F_e\phi_P^{n+1}\right)-\left(I_w^D+I_w^C-F_w\phi_P^{n+1}\right)+\left(I_n^D+I_n^C-F_n\phi_P^{n+1}\right)-\left(I_s^D+I_s^C-F_s\phi_P^{n+1}\right)=S_\phi\delta v \tag{9}$$

By substituting convected flux with equivalent flux, the components of matrix of coefficients will be positive and the matrix will become diagonal:

$$\begin{aligned}I_e^C&=I_e^{CU}-\left(I_e^{CU}-I_e^C\right)\\ I_w^C&=I_w^{CU}-\left(I_w^{CU}-I_w^C\right)\\ I_n^C&=I_n^{CU}-\left(I_n^{CU}-I_n^C\right)\\ I_s^C&=I_s^{CU}-\left(I_s^{CU}-I_s^C\right)\end{aligned} \tag{10}$$

That I^{CU} is the convected flux in upwind scheme. Equation 11 will be obtained with substituting Eq. 10 in Eq. 9:

$$\delta v\frac{\rho_p^n\left(\phi_P^{n+1}-\phi_P^n\right)}{\Delta t}+\left(I_e^D+I_e^{CU}-\left(I_e^{CU}-I_e^C\right)-F_e\phi_P^{n+1}\right)-\left(I_w^D+I_w^{CU}-\left(I_w^{CU}-I_w^C\right)-F_w\phi_P^{n+1}\right)+\left(I_n^D+I_n^{CU}-\left(I_n^{CU}-I_n^C\right)-F_n\phi_P^{n+1}\right)-\left(I_s^D+I_s^{CU}-\left(I_s^{CU}-I_s^C\right)-F_s\phi_P^{n+1}\right)=S_\phi\delta v \tag{11}$$

With a little change it will be acquired:

$$\delta v\frac{\rho_p^n\left(\phi_P^{n+1}-\phi_P^n\right)}{\Delta t}+\left(I_e^D+I_e^{CU}-F_e\phi_P^{n+1}\right)-\left(I_w^D+I_w^{CU}-F_w\phi_P^{n+1}\right)+\left(I_n^D+I_n^{CU}-F_n\phi_P^{n+1}\right)-\left(I_s^D+I_s^{CU}-F_s\phi_P^{n+1}\right)=S_\phi\delta v+\underbrace{\left[\left(I_e^{CU}-I_e^C\right)-\left(I_w^{CU}-I_w^C\right)+\left(I_n^{CU}-I_n^C\right)-\left(I_s^{CU}-I_s^C\right)\right]}_{b_{dc}} \tag{12}$$

With above assumption, the final form of the discretization is as:

$$a_P\phi_P=a_E\phi_E+a_W\phi_W+a_N\phi_N+a_S\phi_S+b_{dc}+S'_\phi \tag{13}$$

That:

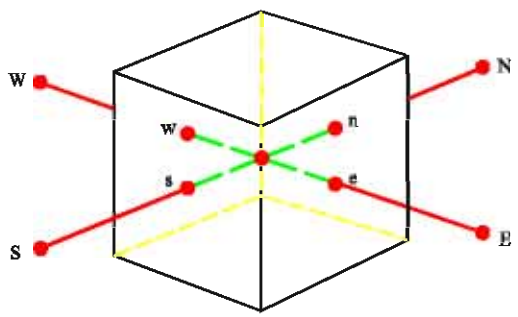

Fig. 1: Finite volume and storage arrangement

$$\begin{aligned} a_E &= D_e + \max(-F_e, 0) \\ a_W &= D_w + \max(F_w, 0) \\ a_N &= D_n + \max(-F_n, 0) \\ a_S &= D_s + \max(F_s, 0) \\ a_P &= a_E + a_{W+} a_{N+} a_S \end{aligned} \tag{14}$$

Depending on flow direction, the b_{d_x} for x direction should be calculated as:

$$\left.\begin{aligned} &\rightarrow F_e\phi_p - f_e - F_w\phi_W + f_w \\ &\leftarrow F_e\phi_E - f_e - F_w\phi_P + f_w \end{aligned}\right\} f_w - f_e + \max(F_e, 0)\phi_p - \max(F_w, 0)\phi_W + \min(F_e, 0)\phi_E \tag{15}$$

Convective fluxes: The numerical dissipation term in UNO scheme, similar to another high resolution scheme, has a non-liner dissipation term. This non-liner dissipation term includes two limiters that are shown in this study with g and β. β is applied to limit characteristics values difference on cell surfaces and then this values are used for calculating of g as another limiter. As will be seen, for each cell face, the values related to the three points have been interfered and therefore the accuracy of this scheme will be of second order.

For a non orthogonal mesh, conservative variable vector and convected flux vector in surface of e is shown by Q and F^{ζ} regularly which ζ is the normal vector of surface.

$$Q = \left(\rho, \rho u, \rho v, \rho E\right)^T \tag{16}$$

$$F^{\zeta} = \left(\rho U^{\zeta}, \rho U^{\zeta} u + PG_x^{\zeta}, \rho U^{\zeta} v + PG_y^{\zeta}, \rho U^{\zeta} H\right)^T \tag{17}$$

$$G_x^{\zeta} = y_{ne} - y_{se} \tag{18}$$

$$G_y^{\zeta} = -\left(x_{ne} - x_{se}\right) \tag{19}$$

That u, v, P, H are velocity in direction of x, velocity in direction of y, total pressure and enthalpy, respectively and:

$$U^{\zeta} = \overrightarrow{U}.\overrightarrow{G^{\zeta}} = uG_x^{\zeta} + vG_y^{\zeta} \tag{20}$$

And convected flux in an arbitrary surface of e would be calculated as:

$$F_e = \frac{1}{2}\left(F_E^{\zeta} + F_P^{\zeta} + R_e\phi_e\right) \tag{21}$$

where, $R_e\phi_e$ is a non-liner dissipation term, based on the characteristic field decomposition of the flux difference. The quantity R_e stands for the right eigenvector matrix, while ϕ_e is a vector containing the components of the anti diffusive flux terms. According to Yee *et al.* (1999) a spatially second order upwind formula for the components of ϕ_e is given by:

$$\phi_e^l = \frac{1}{2}\psi\left(a_{i+\frac{1}{2}}^l\right)\left[g_{i+1}^l + g_i^l\right] - \psi\left(a_{i+\frac{1}{2}}^l + \gamma_{i+\frac{1}{2}}^l\right)\alpha_{i+\frac{1}{2}}^l \tag{22}$$

The eigen values of the Jacobin matrix are denoted by a. The spatial increments of the characteristic variables α are obtained by:

$$\alpha_e^l = R_e^l\left(u_E^l - u_P^l\right) \tag{23}$$

It should be mentioned that characteristic variables is preferred to other type of variables because they generate small gradients in discontinuities. Mulder and van Leer (1985) and Lin and Chieng (1991), who carried out extensive numerical experiments found that at least for one dimensional flow, the best accuracy was obtained using the Riemann variables (characteristic variables). This can perhaps be explained by the fact that only one of these variables will undergo a small change through a wave or a contact front, whereas large changes take place in conserved or primitive variables.

For γ one can take (Yee *et al.*, 1999);

$$\gamma_e^l = \frac{1}{2}\frac{\psi\left(a_e^l\right)\left(g_E^l - g_P^l\right)\alpha_e^l}{\left(\alpha_e^l\right)^2 + \varepsilon} \tag{24}$$

where, ε is an arbitrarily small number such as $10^{(-7)}$. The function Ψ is required to prevent non physical solution such as expansion shocks and introduces a small amount of viscosity. Following the suggestion of Harten and Hyman (1983), it is taken as:

$$\psi(z) = \sqrt{\left(\delta + z^2\right)} \tag{25}$$

And $\delta = \frac{1}{16}$

The most important factor in Eq. 22 is the flux limiter, g, which determines the accuracy and TVD property of the scheme. For the present study, the MINMOD limiter due to Harten (1997) is used, thus:

$$
\begin{aligned}
g_p &= \text{MINMOD}\left(s_p^+, s_p^-\right)\\
s_p^+ &= \alpha_e - \frac{1}{2}\beta_e\\
s_p^- &= \alpha_w + \frac{1}{2}\beta_w\\
\beta_e &= \text{MINMOD}\left(\beta_P, \beta_E\right)\\
\beta_w &= \text{MINMOD}\left(\beta_W, \beta_P\right)\\
\beta_W &= \alpha_w - \alpha_{ww}\\
\beta_P &= \alpha_e - \alpha_w\\
\beta_E &= \alpha_{ee} - \alpha_e
\end{aligned}
\tag{26}
$$

Where:

$$
\text{MINMOD}(x,y) = \text{sign}(x).\text{Max}\left(0, \min\left[|x|, y\,\text{sign}(x)\right]\right) \tag{27}
$$

Also, other limiters such as superbee (Roe, 1986) is used:

$$
g_J^l = S.\max\left[0, \min\left(2\left|\alpha^l_{J+\frac{1}{2}}\right|, S.\alpha^l_{J-\frac{1}{2}}\right), \min\left(\left|\alpha^l_{J+\frac{1}{2}}\right|, S.\alpha^l_{J-\frac{1}{2}}\right)\right] \tag{28}
$$

Where: $S = \text{sgn}\left(\alpha^l_{J+\frac{1}{2}}\right)$

The superscript *l* denotes the various characteristic variable.

Solution algorithm: The technique used is the SIMPLE scheme for the steady state problems presented herein. The adapted SIMPLE scheme consists of a predictor and corrector sequence of steps in each iteration. The predictor step solves the implicit momentum equations using the old pressure field. Thus, for example, for the u component of velocity, the momentum predictor stage can be written as:

$$
u^* = H\left(u^*\right) - D\nabla P^0 + S'_u \tag{29}
$$

where, H contains all terms relating to the surroundings nodes and superscripts* and 0 denote intermediate and previous iteration values, respectively. Note that the pressure gradient term in now written out explicitly; it is extruded from the total momentum flux by simple subtraction and addition. The corrector step equation can be written as:

$$
u^{**} = H\left(u^*\right) - D\nabla P^* + S'_u \tag{30}
$$

Hence, from Eq. 29-30,

$$
\begin{aligned}
&u^{**} - u^* = -D\nabla\left(P^{**} - P^*\right)\\
&\text{or}\\
&\delta u = -D\nabla\delta p
\end{aligned}
\tag{31}
$$

Now the continuity equation demands that

$$
\nabla\left(\rho^* u^{**}\right) = 0 \tag{32}
$$

for steady state flows. For compressible flows, it is essential to account for the effect of change of density on the mass flux as the pressure changes. This is accounted for by linearizing the mass fluxes as follows (Karki and Patankar, 1989)

$$
\rho^* u^{**} \approx \rho^0 u^* + \rho^0\delta u + u^*\delta p \tag{33}
$$

Or

$$
\rho^* u^{**} \approx \rho^0 u^* - \rho^0 D\nabla\delta p + u^*\left(\frac{d\rho}{dp}\right)\delta p \tag{34}
$$

where, Eq. 31 is invoked to eliminate δu and δp is related to δp by the appropriate equation of state. Substitution of Eq. 34 into 32 yields a pressure correction equation of the form

$$
A_P.\delta p_P^* = A_E.\delta p_E^* + A_W.\delta p_W^* + A_N.\delta p_N^* + A_S.\delta p_S^* + S_P \tag{35}
$$

where, S_P is the finite difference analog of $\nabla(\rho^{\circ}u^*)$, which vanishes when the solution is converged.

The A coefficients in Eq. 35 take the form (the expression for A_E is given as an example)

$$
A_E = \left(\rho^0\tilde{a}D\right)_e - \lambda_e\left(\tilde{a}u^*\right)_e.\left(\frac{d\rho}{dp}\right)_e \tag{36}
$$

where, λ is a factor whose significance is explained subsequently.

Because the mass flux at a cell face is computed directly (via Eq. 21) from nodal values of ρ_e^0 and u_e^* in Eq. 36 are not readily available. To compute those values, assumptions concerning the variations of ρ need to be made. For example, if upwinding is chosen, then λ would take the value of 1 when u is positive; otherwise it would be zero. Alternatively if a central difference formula is used, then $\lambda = 1/2$ it is important to recognize, however, that such assumption have no influence whatsoever on the final solution because they affect only the pressure correction coefficients and as δp goes to zero at convergence, the solution is, therefore, independent of how those coefficients are formulated; however, they do influence the convergence behavior. What is important is how $\nabla(\rho u^*)$ in Eq. 35 is computed (as this does determine the solution) and this is based on the UNO principle outlined earlier.

The structure of the coefficients in Eq. 35 simulates the hyperbolic nature of the equation system. Indeed a

closer inspection of expression Eq. 36 would reveal an upstream bias of the coefficients (A decreases as u increases) and this bias is proportional to the square of the Mach number. Also note that the coefficients reduce identically to their incompressible form in the limit of zero Mach number.

The overall solution procedure follows the same steps as in the standard SIMPLE algorithm, with the exception of solving the hyperbolic like pressure correction Eq. 33. To ensure convergence of the iterative process, under relaxation factors between 0.1 and 0.2 for pressure correction and between 0.2 and 0.5 for the other variables are employed.

Boundary conditions: At the inlet of the domain, all flow variables are specified if the flow is supersonic. For subsonic inlet flow, only three of the four variables need to be prescribed: the total temperature, the angle of attack and the total pressure. The pressure is obtained by zeroth order extrapolation form interior points. At outlet, all of the flow variables are obtained by linear extrapolation for supersonic velocities, the pressure is fixed when the outlet is subsonic. Slip boundary conditions are used on the lower and upper walls of the bump in the inviscid flow test cases.

Also, numerical boundary conditions have to be formulated for the flux limiters. According to Yee (1986) there are three choices of boundary values for the g_i^l function in Eq. 20. In the present study, the g_i^l function on a boundary face has been approximated by $\alpha^l_{i+\frac{3}{2}}$, which has the smallest dissipative value among the three possible choices.

RESULTS AND DISCUSSION

In the first test, the results of steady transonic flow with inlet Mach number of 0.675 over a 10% thick bump for grids 98*26 are calculated. Figure 2 shows the geometry of the 10% thick bump. In this case, the superbee limiter is used for both UNO and TVD schemes. Figure 3a and c show the Mach number and pressure

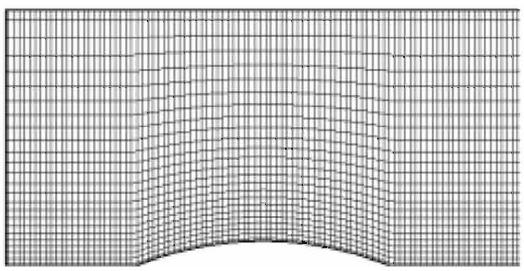

Fig. 2: Geometry

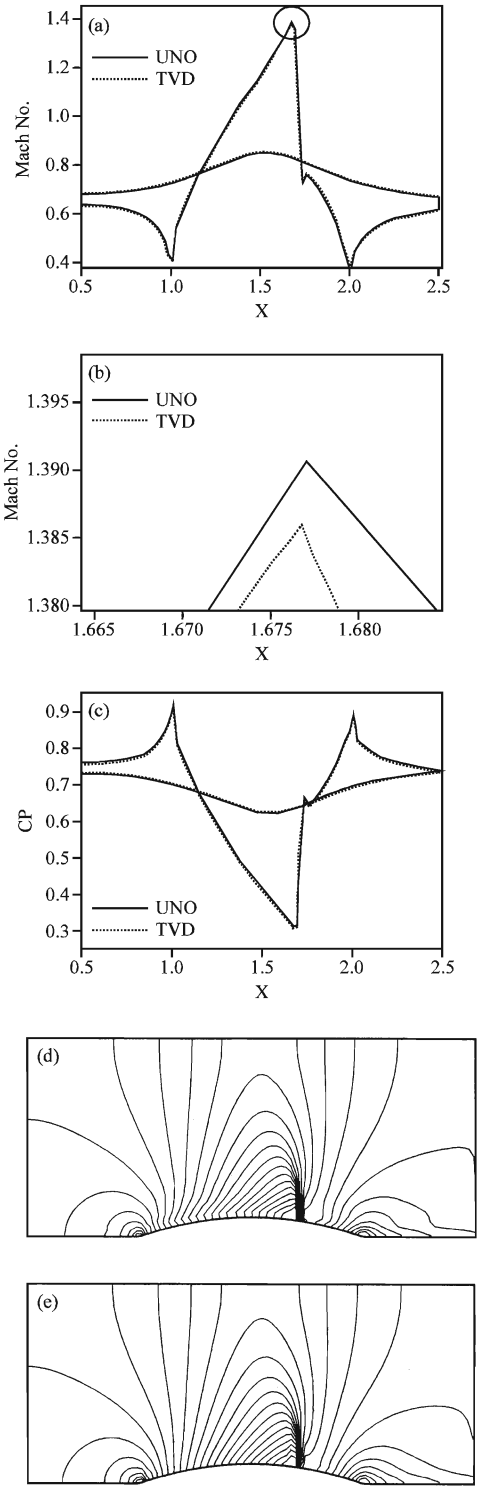

Fig. 3: Transonic flow over 10% thick bump, inlet M_∞ = 0.675, (a) Mach number distribution, (b) Focus on Mach number, (c) Pressure ratio, (d) Mach contour UNO scheme and (e) Mach contour in TVD scheme

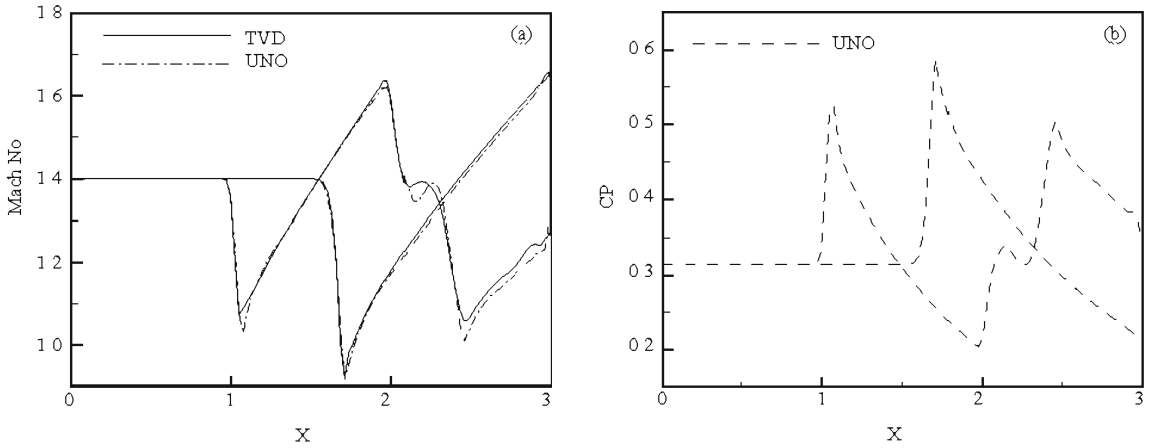

Fig. 4: Supersonic flow over 4% thick bump, inlet $M_\infty = 1.4$, (a) Mach number distribution and (b) Pressure ratio on lower and upper wall

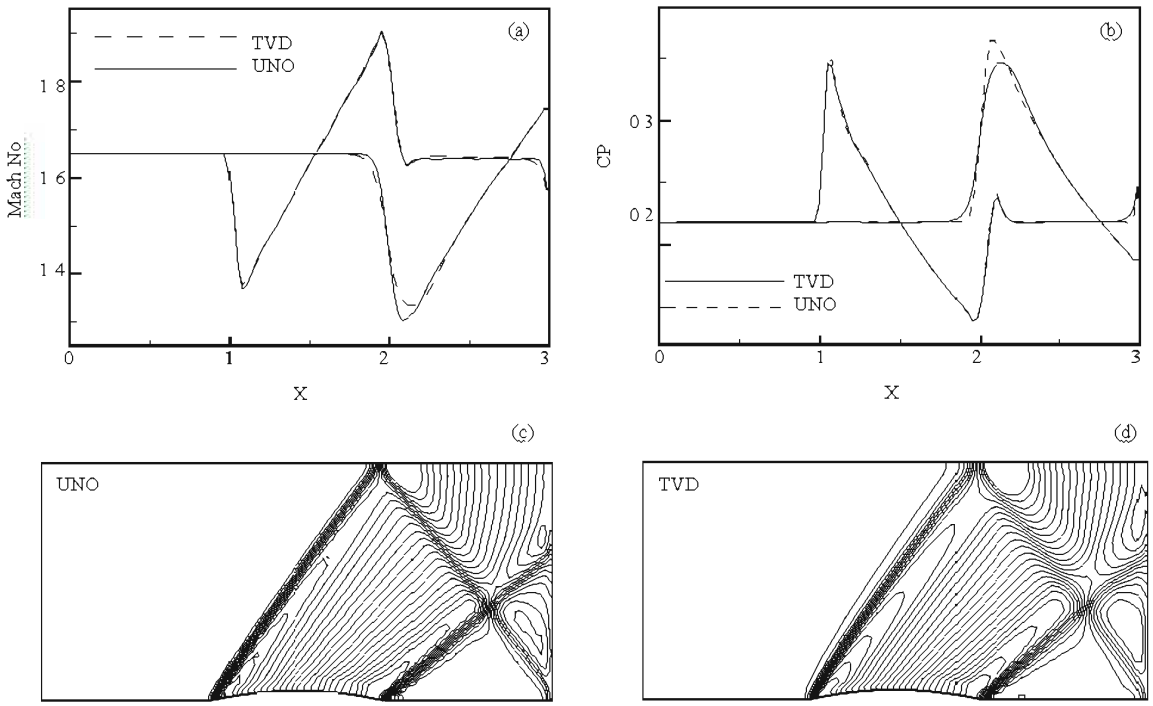

Fig. 5: Supersonic flow over 4% thick bump, inlet $M_\infty = 1.65$, (a) Mach No distribution, (b) Pressure ratio, (c) Mach contour in UNO scheme and (d) Mach contour in TVD scheme

coefficient distribution on the lower and upper walls for two schemes. Figure 3b shows precisely the maximum point in Mach number distribution for both UNO and TVD scheme. This comparison is presented that the shock predicted by the UNO scheme is better than the TVD scheme. Figure 3d and e show Mach contour distribution for UNO and TVD scheme, respectively. In general, the results nearly are the same in transonic flow.

The second case is supersonic flow over 4% thick bump on a channel wall. The computations were performed on a grid 90*30. The results of supersonic flow with inlet Mach number equal to 1.4 are shown in Fig. 4. The Mach number and pressure ratio distribution on the upper and lower surfaces for present scheme are compared with the TVD (Issa and Javareshkian, 1998) prediction. The agreement between the two solutions is remarkable, thus verifying the validity of the UNO scheme in pressure-based algorithm.

The third case is supersonic flow in the previous case with inlet Mach number equal to 1.65. Figure 5a and b

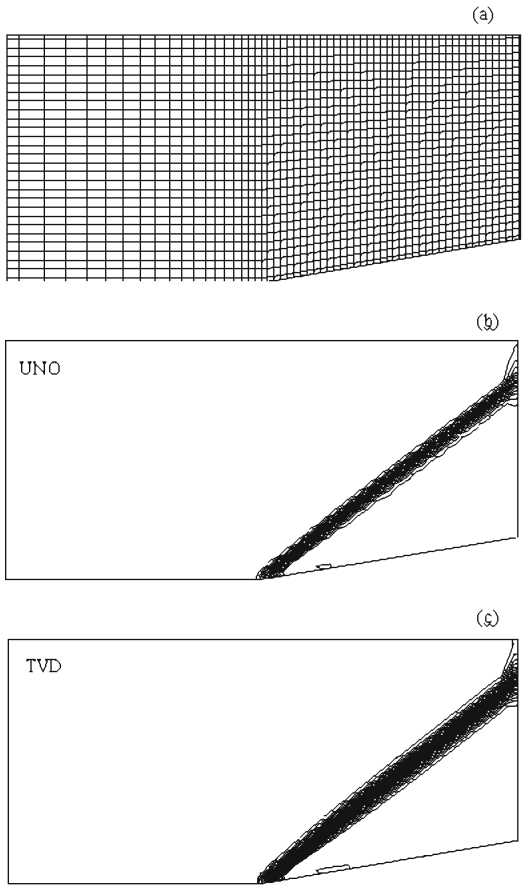

Fig. 6: Supersonic flow over 4% ramp 10%, inlet $M_\infty = 2.0$, (a) Geometry, (b) Mach contour in UNO scheme and (c) Mach contour in TVD scheme

shows the Mach number and pressure coefficient distribution on the upper and lower surface for both UNO and TVD schemes. According to the Fig. 5a, the reflection of leading edge shock at the upper wall for UNO scheme, is sharper than TVD scheme. Also for the lower wall, after reflection shock, near the outlet, Mach number distribution has been smeared in TVD scheme. In more accurate view, after reflection shock at the lower wall, there is a little under shoot for TVD scheme. Figure 5c and d show Mach contour distributions for both UNO and TVD schemes. The results show near the shock, UNO Mach contour, is more compact and precise than TVD Mach contour.

The fourth case is supersonic flow over a 10 deg ramp. The computations were performed on a grid 60*30 (Fig. 6a) and inlet Mach is 2.0. The Mach contours for both UNO and TVD schemes are presented in

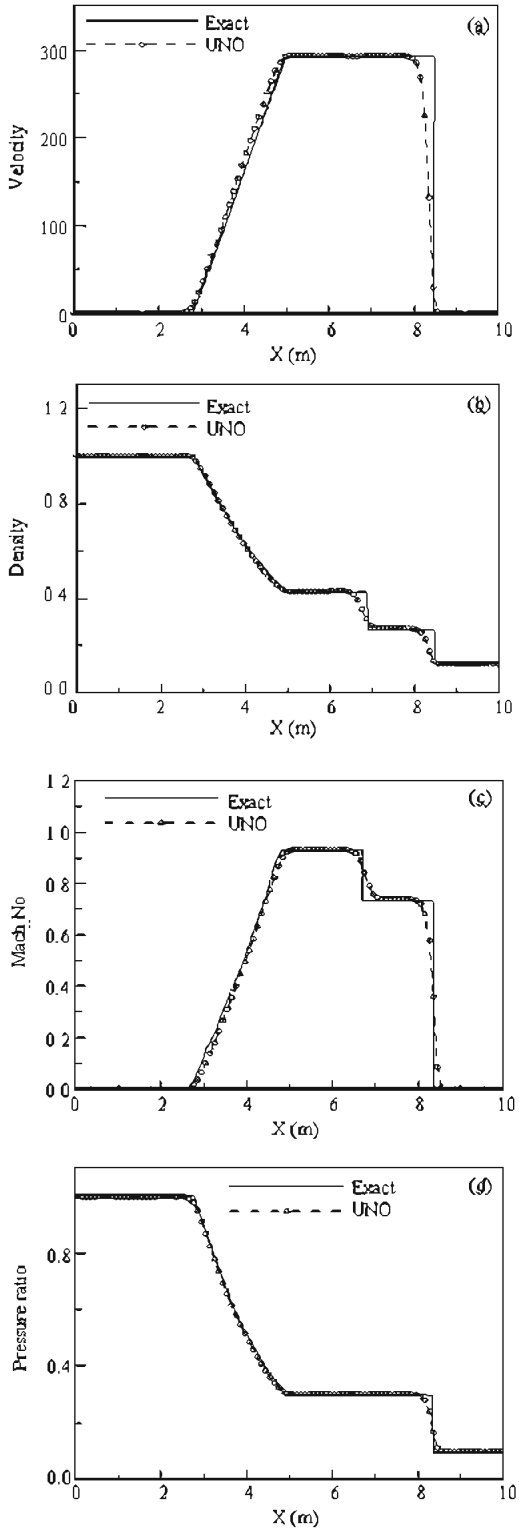

Fig. 7: Shock-tube results for an initial pressure ratio $P_H/P_L = 10$ at time $t_0 = 6.0$, (a) Velocity, (b) Density, (c) Mach number and (d) Pressure ratio distribution

Fig. 6b and c, respectively. As it can bee seen, the shock contours for UNO scheme are more compact and precise than TVD scheme.

The fifth case is one-dimensional transient shock tube problem. Figure 7a-d show the spatial distribution of velocity, density, Mach number and pressure ratio, respectively, along the shock tube at a given instant in time in a shock-tube for an initial pressure of 10. The results of computation on a mesh of 100 nodes are compared with the analytic solution. It can be seen that the shock is sharply captured and the contact discontinuity is resolved and oscillation is not relatively produced for the UNO scheme.

CONCLUSION

A pressure based implicit procedure has been described that incorporates bounded high resolution of discontinuities and is, therefore, well suited to all flow ranging from subsonic to supersonic. The boundedness criteria for this procedure are determined from UNO schemes, which are applied to the fluxes of the convected quantities, including mass flow. The flux limiter is based on the characteristic variables. The main findings can be summarized as follows:

- The agreement between the results of the present implementation of UNO schemes and TVD schemes is excellent, as it should be
- The UNO schemes based on characteristic variable produces more smooth solution around discontinuities than TVD scheme

ACKNOWLEDGMENT

The authors are grateful to the deanship of Mechanic Engineering Department, University of Tabriz for their financial support.

REFERENCES

Boris, J.P. and D.L. Book, 1997. Flux-corrected transport. Minimal error FCT algorithms. J. Comput. Phys., 135: 172-186.

Capdeville, G., 2008a. A Hermit upwind WENO scheme for solving hyperbolic conservations laws. J. Comput. Phys., 227: 2430-2454.

Capdeville, G., 2008b. A central WENO scheme for solving hyperbolic conservations laws on non uniform-meshes. J. Comput. Phys., 227: 2977-3014.

Colella, P. and M.D. Sekora, 2008. A limiter for PPM that preserves accuracy at smooth extrema. J. Comput. Phys., 227: 7069-7076.

Druguet, M.C. and D.E. Zeitoun, 2003. Influence of numerical and viscous dissipation on shock wave reflections in supersonic steady flows. J. Comput. Fluids, 32: 515-533.

Harten, A. and J.M. Hyman, 1983. Self adjusting grid methods of one dimensional hyperbolic conservation laws. J. Comput. Phys., 50: 235-269.

Harten, A., 1997. High resolution scheme for hyperbolic conservation laws. J. Comput. Phys., 135: 260-278.

Harten, A., B. Engquist, S. Osher and S.R. Chakravarthy, 1997. Uniformly high order accurate essentially non-oscillatory schemes. J. Comput. Phys., 131: 3-47.

Issa, R.I. and M.H. Javareshkian, 1998. Pressure_based compressible calculation method utilizing total variation diminishing schemes. AIAA. J., 36: 1652-1657.

Karki, K.C. and S.V. Patankar, 1989. Pressure-based calculation procedure for viscous flows at all speeds in arbitrary configurations. AIAA. J., 27: 1167-1174.

Kim, K.H. and C. Kim, 2005. Accurate, efficient and monotonic numerical methods for multi- dimensional compressible flows-partII; Multi-dimensional limiting process. J. Comput. Phys., 208: 570-615.

Kumar, R. and M.K. Kadalbajoo, 2008. A class of high resolution shock capturing schemes for hyperbolic conservation laws. J. Applied Math. Comput., 195: 110-126.

Lian-Xia, L., L. Hua-Sheng and Q.L. Jian, 2008. An improved r-factor algorithm for TVD schemes. J. Heat Mass Transfer, 51: 610-617.

Lin, H. and C.C. Chieng, 1991. Characteristic-based flux limiters of an essentially third-order flux-splitting method for hyperbolic conservation laws. J. Numerical Methods Fluid, 13: 232-246.

Mandal, J.C. and J. Subramanian, 2008. On the link between weighted least-squares and limiters used in higher-order reconstructions for finite volume computations of hyperbolic equations. J. Applied Numerical Math., 58: 705-725.

Mulder, W.A. and B. van Leer, 1985. Experiments with implicit upwind methods for the Euler equations. J. Comput. Phys., 59: 232-246.

Roe, P.L., 1986. Characteristic-based schemes for the euler equations. Ann. Rev. Fluid Mech., 18: 337-337.

Roe, P.L., 1997. Approximate riemann solvers, parameter vectors and difference schemes. J. Comput. Phys., 135: 250-258.

Shen, Y., Y. Guowei and G. Zhi, 2006. High-resolution finite compact difference scheme for hyperbolic conservation laws. J. Comput. Phys., 216: 114-137.

Shu, C.W. and S. Osher, 1989. Efficient implementation of essentially non-oscillatory shock capturing schemes. J. Comput. Phys., 83: 32-78.

Sohn, S.I., 2005. A new TVD-MUSCL scheme for hyperbolic conservation laws. J. Comput. Math. Appl., 50: 231-248.

Sokolov, I.V., K.G. Powell, T.I. Gombosi and I.I. Roussev, 2006. A TVD principle and conservative TVD schemes for adaptive *Cartesian grids*. J. Comput. Phys., 220: 1-5.

Titarev, V.A. and E.F. Toro, 2005. WENO scheme based on upwind and centred TVD fluxes. J. Comput. Fluids, 34: 705-720.

Van Leer, B., 1997. Towards the ultimate conservative difference scheme V: A Second-order sequel to Godunov's Sequel. J. Comput. Phys., 135: 229-248.

Yee, H.C., 1986. Numerical experiments with a systematic high-resolution shock-capturing scheme. NASA TM-88325.

Yee, H.C., N.D. Sandham and M.J. Djomehri, 1999. Low-dissipative high-order shock-capturing methods using characteristic-based filters. J. Comput. Phys., 150: 199-238.